Assessment of Synthetic Aperture Radar (SAR) and Optical Remote Sensing Data in Aboveground Carbon Stock Estimation of Coconut (Cocos nucifera L.) in Butuan City

Gracelle W. Antiporda
Department of Geodetic Engineering

Karla Marie E. Bernaldez
Department of Geodetic Engineering

Jun Love E. Gesta
Department of Geodetic Engineering

https://doi.org/10.5109/7323265

出版情報：Proceedings of International Exchange and Innovation Conference on Engineering & Sciences (IEICES). 10, pp.211-218, 2024-10-17. International Exchange and Innovation Conference on Engineering & Sciences
バージョン：

Assessment of Synthetic Aperture Radar (SAR) and Optical Remote Sensing Data in Aboveground Carbon Stock Estimation of Coconut (*Cocos nucifera* L.) in Butuan City

Gracelle W. Antiporda[1], Karla Marie E. Bernaldez[1], Jun Love E. Gesta[1,2]
[1]Department of Geodetic Engineering, [2]Caraga Center for Geo-Informatics,
College of Engineering and Geosciences, Caraga State University, Butuan City, 8600, Philippines
corresponding author email: jlegesta@carsu.edu.ph

Abstract: *Evaluating aboveground biomass (AGB) assists foresters and scientists in comprehending and monitoring ecosystem responses and contributions to the global carbon cycle, climate change, and terrestrial carbon accounting. Traditional approaches, such as the destructive method, are the most accurate; however, they are often expensive and inefficient, which favors the remote sensing approach because of its convenience. This study assessed remote sensing datasets, which are Synthetic Aperture Radar (SAR) and Optical Remote Sensing, to gauge the AGB of coconut trees and their carbon storage. Employing Multi-linear Regression with 33 variables led to several AGB models, among which Model 3 stood out for its excellent balance of coefficient of determination (R^2) and Root Mean Square Error (RMSE) values. Results estimated that the aboveground carbon stock of coconut trees is 13 megagrams of carbon per hectare (MgC/ha) with an RMSE of 2.345 MgC/ha. These findings' efficiency and accuracy demonstrate that integrating multiple satellite sensors creates more reliable AGB and carbon stock estimations.*

Keywords: *Cocos nucifera* L., Coconut, correlation, Optical images, SAR.

1. INTRODUCTION

Climate change is the long-term shift in the climate's weather patterns and average annual temperatures [1,2], and greenhouse gases (GHG) play a significant role in maintaining the planet warm enough to inhabit. However, a large amount of greenhouse gases has accumulated in lower layers of the atmosphere, causing the Earth's climate to change rapidly [2]. The build-up of carbon dioxide and other greenhouse gases in the atmosphere traps and contributes to climate change, which disturbs carbon sequestration [3]. It is evident that forests play an important role in regulating Earth's climate, serving as carbon sinks that store twenty-five (25) percent of human-generated carbon emissions each year [4]. In 2011, the Philippine Forest estimated 644 million metric tons of carbon stocks in living forest biomass, which sequestered 1.3% of the country's GHG emissions [5].

Given its tropical climate, the Philippines offers ideal conditions for palm trees to flourish, with warm temperatures, high humidity, and abundant moisture. As a result, forests in the Philippines contain palm trees, and palms are among the most extensively cultivated plant families. They hold the utmost significance in the plant kingdom due to their immense usefulness to man and their resilience to climate change [6,7]. Coconut (*Cocos nucifera* L.) [8] is among the palm trees in the Philippines that hold significance not only for their usefulness to man but also to the environment. Coconut plantation provides several ecosystem services and is one of the major agricultural sectors in the Philippines [9]. Notably, the Philippines is one of the top producers of coconut products, supplying over 92 countries worldwide [10]. Coconut trees are referred to as the tree of life, contributing to the basic necessities of human life, providing not just as a source of food and shelter but also contributing to withstanding natural phenomena [11]. Lastly, coconut has the potential to play a significant role in addressing climate change by sequestering a considerable amount of carbon, which is considered the most stable carbon store due to its perennial nature and minimal residue burning compared to crops like rice and sugarcane [12].

Accurate estimates of aboveground biomass enable the assessment of carbon productivity and sequestration [13], which is essential for global carbon budgeting and monitoring forest ecosystems [14]. The traditional method of aboveground biomass is the most accurate but labor-intensive and time-consuming, which favored the remote sensing approach because of its convenience [15]. Remote sensing technologies offer effective tools for monitoring and understanding Earth and its environmental systems [16]. Satellite-based estimation of AGB and carbon stocks has become more accessible, offering varied spectral, spatial, and temporal resolutions for estimating biomass, selected based on accessibility, effectiveness, and expense. Over the years, Synthetic Aperture Radar (SAR) data gained popularity because of its ability to penetrate areas prone to cloud cover. Also, the use of optical remote sensing data for forest biomass estimation has been widely used because of its spatial and temporal conditions.

The combination of SAR with Sentinel-2 imagery has been advocated to harness the strengths of both radar and optical remote sensing techniques, particularly in tropical regions where cloud cover and canopy density pose significant challenges [17]. Also, there is limited information on estimating the AGB and carbon stock of this palm tree using remote sensing technologies. This study will fill in the information gap by estimating and mapping the AGB and carbon stock of coconut trees in Butuan City, Agusan del Norte, through the assessment of bands and the synergistic use of Sentinel-1 and Sentinel-2 data.

2. METHODOLOGY

2.1 Study Area

The study was conducted in Butuan City (see Fig. 1), Agusan del Norte, Philippines. Geographically, it is situated at approximately 8°57' North, 125°32' East, on the island of Mindanao. The city's existing land use consists of agriculture, forestland, pastureland, commercial, and residential [18]. The city also boasts a thriving coconut industry in the Caraga region. The presence of these plant species not only underscores the city's agricultural potential but also its ecological diversity.

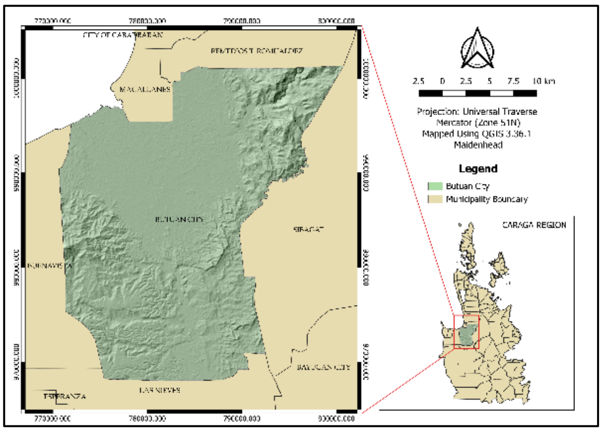

Fig. 1. Map of Butuan City.

2.2 Boundary Demarcation

Sentinel-2 image acquired on August 04, 2023, was utilized for the demarcation of coconut. Cloud masking procedures were implemented to address the presence of clouds, which could potentially interfere with accurate classification. Employing a Supervised Vector Machine (SVM) [19] for image classification, initial classification output was generated and subjected to accuracy assessment. Feature extraction was conducted from the classified image and then manually refined in Google Earth to rectify misclassifications, particularly concerning coconut.

2.3 Development of Aboveground Biomass Model using Field Measured Aboveground Biomass and Sentinel Backscatter Images

2.3.1 Field Data Collection

The estimation of aboveground biomass for palm species commenced with the establishment of 20 x 20-meter sample plots within the study site, selected randomly to ensure representative sampling. A total of 40 plots were designated for coconut plantations. Subsequently, for the development of the aboveground biomass model, twenty-eight (28) plots were randomly allocated, leaving twelve (12) plots reserved for accuracy assessment or model validation. The stochastic nature of plot selection resulted in an uneven distribution of representative plots across species. Field measurements were conducted from December 14, 2023, to January 20, 2024. During the fieldwork phase, the tree height was measured using a hypsometer (see Table 1). These measurements were crucial for estimating aboveground biomass using specific allometric equations tailored to coconut. All trees within the plots were carefully accounted for, and the coordinates of plot corners were recorded to accurately pinpoint plot centers. Moreover, handheld global positioning system (GPS) receivers (see Table 1) were employed to document the geographic coordinates of sampling points.

Table 1. Equipment used in the field data collection.

Equipment	Image
Hypsometer Model: Haglof Vertex Laser Geo Brand: Haglöf Sweden Origin: Sweden Source: https://haglofsweden.com/project/laser-geo-2/	
Handheld global positioning system (GPS) receiver Model: Oregon® 750 Brand: Garmin Origin: United States Source: https://www.garmin.com/en-US/p/550462	

2.3.2 Allometric Equation for Aboveground Biomass and Carbon Stock Estimation

Specific allometric equations were employed to estimate the aboveground biomass. The equation developed by Hairiah et al. [20] for coconut, denoted as Equation 1, was utilized.

$$AGB = 4.5 + 7.7 * H \qquad \text{Equation 1}$$

where:

AGB = Aboveground biomass (kg/tree)
H = tree height (m)

The equation mentioned above was applied to each individual tree within the established plot, and the resulting values were summed to determine the aboveground biomass (AGB) of each plot, expressed in tons per plot. Furthermore, the estimated AGB values obtained from the equations were converted into carbon stock for individual trees using a conversion factor of 47% of the dry biomass, as recommended by Effendi et al. [21]. By default, this conversion factor is presumed to represent the carbon content of all segments of the tree. The equation for calculating carbon stock is provided below.

$$CS = Total\ AGB * 0.47 \qquad \text{Equation 2}$$

where:

CS = Carbon Stock (ton/plot)
Total AGB = Aboveground biomass (ton/plot)

2.3.3 Satellite Data Acquisition and Pre-Processing

The Sentinel-1A images and Sentinel-2 images at level-2A, encompassing 13 spectral bands, utilized in this study were obtained from the European Space Agency's (ESA) Data Hub. The Sentinel-1A images, collected on August 06, 2023, were acquired in Ground Range Detected (grd) processing level and in Interferometric Wide Swath Mode of VH (vertical transmit-horizontal receive) and VV (vertical transmit-vertical receive) polarization; these images were preprocessed using Sentinel Application Platform (SNAP) Software. Mosaicking was performed after sub-setting the images to reduce file size and processing time, focusing on the study area. Preprocessing was performed, including applying orbit files and radiometric calibration to ensure accurate satellite data and converting digital number values to Sigma naught values, followed by speckle filtering using refined Lee speckle filter [22], geometric correction using a 10-meter resolution Digital Elevation Model (DEM), transforming pixel values to decibels, and spatial resampling from 10 meters to 20 meters to match field plot sizes and the Sentinel-2 image.

Furthermore, to incorporate textural information from the images, the Grey Level Co-occurrence Matrix (GLCM), a statistical method, was utilized as a predictor variable. GLCM analyses pixel pair properties over a specific distance and orientation, which effectively captures the spatial dependence between spectral values, allowing for a detailed assessment of vegetation patterns and densities [23]. A total of 8 grey level co-occurrence matrices (see Table 2) were generated using SNAP software, enhancing the analysis of image texture characteristics.

Table 2. Sentinel-1 Predictor Variables.

Backscatter Polarization	**Description**
VV	Vertical transmit - Vertical receive
VH	Vertical transmit - Horizontal receive
VV+VH	Vertical transmit - Vertical receive + Vertical transmit - Horizontal receive
GLCM	
VV_Mean	Vertical transmit - Vertical receive Mean
VV_Variance	Vertical transmit - Vertical receive Variance
VV_Contrast	Vertical transmit - Vertical receive Contrast
VV_Dissimilarity	Vertical transmit - Vertical receive Dissimilarity
VH_Mean	Vertical transmit - Vertical receive Mean
VH_Variance	Vertical transmit - Vertical receive Variance
VH_Contrast	Vertical transmit - Horizontal receive Contrast
VH_Dissimilarity	Vertical transmit - Vertical receive Dissimilarity

Sentinel-2 images at level-2A with reflectance data were utilized to mitigate atmospheric influences on the reflected wavelengths, ensuring accurate derivation of the desired indices. The spectral reflectance of the 20-meter bands served as predictors for AGB estimation (see Table 3), aligning with the nominal size of the Sentinel-1 images and field plots. To incorporate additional predictors, bands with 10- and 60-meter resolutions were resampled to 20-meter resolution. Moreover, six vegetation indices and four biophysical variables were generated to evaluate their correlation with AGB. The four biophysical variables, which are Leaf Area Index (LAI), Fraction of Absorbed Photosynthetically Active Radiation (FAPAR), Chlorophyll Content (CAB), and Canopy Water Content (CW), are crucial for estimating biomass.

LAI is significant in quantifying canopy structure and understanding plant growth [24]. FAPAR, the fraction of the incoming solar radiation absorbed by green parts of the canopy for photosynthesis, is a critical variable in modeling vegetation primary productivity and is a direct indicator of energy absorption [25]. CAB, which measures the chlorophyll content, is essential for assessing plant health, as chlorophyll plays a central role in the photosynthesis process [24]. Lastly, CW estimates the equivalent water thickness of a vegetation canopy, which is essential for assessing plant water stress and can affect the accuracy of other vegetation indices [26]. These biophysical variables, often retrieved from satellite imagery, are used in various models to estimate biomass, and models leveraging these variables have demonstrated significant potential in estimating above-ground biomass in different ecosystems; studies have shown that integrating LAI, FAPAR, and other related indices from Sentinel-2 imagery can effectively predict forest biomass and enhance the accuracy of ecological models [25,27].

Table 3. Sentinel-2 Predictor Variables.

Multispectral Bands	**Description**
B1	Coastal Aerosol (443 nm)
B2	Blue (490 nm)
B3	Green (560 nm)
B4	Red (665 nm)
B5	Vegetation Red Edge (705 nm)
B6	Vegetation Red Edge (740 nm)
B7	Vegetation Red Edge (783 nm)
B8	Near-Infrared (842 nm)
B8A	Vegetation Red Edge (865 nm)
B9	Water Vapor (945 nm)
B11	Short Wave Infrared (1.610 nm)
B12	Short Wave Infrared (2.190 nm)
Biophysical Variables	**Description**
LAI	Leaf Area Index
CAB	Chlorophyll Content in the leaf
CW	Water Content
FAPAR	Fraction of Absorbed Photosynthetically Active Radiation
Vegetation Indices	**Mathematical Formula**
NDVI	(NIR- R)/ (NIR+ R)
NDI45	(NIR- R)/ (NIR+ R)
IRECI	(NIR − R)/(RE1/RE2)
TNDVI	[(NIR- R)/ (NIR+ R) + 0.5] 1/2
SAVI	((NIR- R)/ (NIR+ R) + 0.5) * 1.5
S2REP	705 + 35 * ((((NIR + R)/2) − RE1)/ (RE2 − RE1))

2.3.4 Extraction of Pixel Values of Sentinel-1 and Sentinel-2 Predictor Variables

Pixel values were extracted for each variable from both Sentinel-1 and Sentinel-2 images, utilizing the center coordinates of the plots (latitude, longitude) as references. For the Sentinel-1 image, a total of 11 variables were utilized. For Sentinel-2, pixel values were extracted from bands, vegetation indices, and biophysical variables, totaling 22 predictor variables. Subsequent statistical analysis was conducted using SPSS and Microsoft Excel. Multiple Linear Regression (MLR) was employed to model AGB using the predictor variables from both Sentinel-1 and Sentinel-2 imagery.

Four models were created: Model 1 represented the Sentinel-1 variables, Model 2 represented the Sentinel-2 variables, Model 3 combined data from both Sentinel-1 and Sentinel-2, and Model 4 is the highest variable that correlated from either Sentinel-1 or Sentinel-2. The coefficient of determination (R^2) and the Root Mean Square Error (RMSE) were calculated to assess the accuracy of the AGB models derived from MLR. An assessment was conducted using the twelve (12) validation plots to validate the accuracy of the AGB and Carbon Stock Maps. The RMSE between the field measured AGB and calculated carbon stock, compared with the predicted AGB and carbon stock, were computed to evaluate the model's performance. The equation for RMSE is depicted in Equation 3.

$$RMSE = \sqrt{\frac{1}{n}\sum_{i=1}^{n}(y_i - \hat{y}_i)^2} \qquad \text{Equation 3}$$

where:

n = total number of observations,
y_i = actual value of an observation,
$\hat{y}_i$ = predicted value of that observation.

3. RESULTS AND DISCUSSIONS

3.1 Demarcation of Palm Trees

The boundary demarcation of coconut in Butuan City using image classification and Google Earth refinement is shown in Fig. 2. The total area was calculated to be approximately 7,864 hectares.

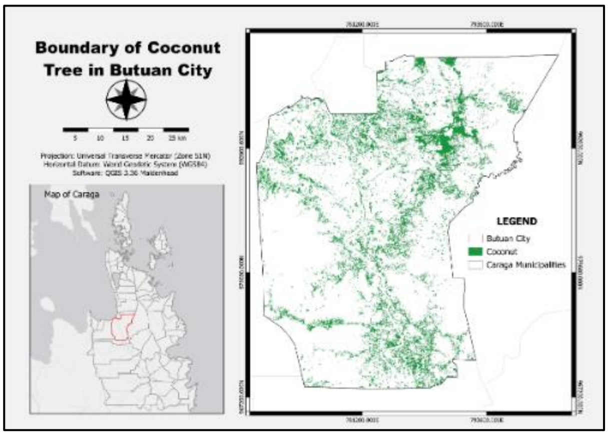

Fig. 2. Boundary of coconut trees in Butuan City.

3.2 Correlation of Sentinel-1 variable with Field Measured AGB

Sentinel-1 predictor variables were categorized into backscatter polarizations and grey-level co-occurrence matrix variables. The correlation of Sentinel-1 predictor variables with field-measured AGB ranged from -0.034 to 0.540 (see Table 4), indicating a moderate relationship. Among the seven variables, three demonstrated significant relationships, with the VH polarization exhibiting a noteworthy correlation at the 0.05 significance level, with a correlation coefficient of 0.540.

Table 4. Summarize Correlation Coefficient of Sentinel-1 predictor variables.

Predictor Variables	R^2
VV	-0.297
VH	0.021
VV_VH	-0.184
VV_Contrast	-0.034
VV_Dissimilarity	-0.102
VV_GLCMMean	0.190
VV_GLCMVariance	0.168
VH_Contrast	$.540^{**}$
VH_Dissimilarity	$.492^{**}$
VH_GLCMMean	0.354
VH_GLCMVariance	$.377^{*}$

* Correlation is significant at the 0.05 level (2-tailed).
** Correlation is significant at the 0.01 level (2-tailed).

3.3 Correlation of Sentinel-2 variable with Field Measured AGB

The correlation of Sentinel-2 predictor variables with field-measured AGB for coconut ranged from -0.020 to 0.391, as shown in Table 5. The table presents correlations of coefficients between predictor variables and AGB measurements in coconut fields. Significant correlations (*$p < 0.05$, **$p < 0.01$) indicate that certain spectral bands (i.e., B11, B12, B6, B7,) and biophysical variables (i.e., CW, FAPAR) show relationships with AGB. These findings suggest that these remote sensing metrics could be reliable indicators for estimating biomass in coconut trees.

Table 5. Summarized Correlation Coefficient of Sentinel-2 predictor variables.

Predictor Variables	R^2
B1	-0.257
B11	$-.620^{**}$
B12	$-.397^{*}$
B2	-0.117
B3	-0.206
B4	-0.115
B5	-0.333
B6	-0.240
B7	-0.153
B8	-0.183
B8A	-0.097
B9	-0.024
NDVI	-0.020
NDI45	0.020
IRECI	0.111
TNDVI	-0.013
SAVI	0.008
S2REP	0.236
LAI	0.200
CAB	0.258
CW	0.389^{*}
FAPAR	0.391^{*}

* Correlation is significant at the 0.05 level (2-tailed).
** Correlation is significant at the 0.01 level (2-tailed).

3.4 Aboveground Biomass Model Development

Table 6 consists of allometric models' parameters developed to estimate the AGB of coconut trees using remote sensing data from Sentinel-1 and Sentinel-2 satellites. Only sentinel predictor variables showing significant correlation with the field measured AGB were considered for modeling the AGB predictive formula. The AGB predictive model relied on the multilinear regression analysis, aiming to attain the highest coefficient of determination (R^2) and lowest RMSE. Model 1 exhibited moderate predictive power for coconut ($R^2 = 0.34$) with a significant p-value of 0.017, suggesting a reasonably good fit. RMSE was moderate, with 0.220, indicating average prediction error. Model 2 had a high R^2 value, which is 0.69, with strong statistical significance ($p < 0.001$), implying a robust model for coconut biomass prediction. Model 3 showed excellent performance with R^2 of 0.72 and a significant p-value of <0.001. Lastly, model 4 had a strong R^2 equal to 0.38 with a highly significant p-value of <0.001.

Based on the results of the models developed for estimating the AGB of coconut trees using SAR and optical remote sensing data, it is evident that model 3 is suitable for generating the AGB. Model 3, which combines Sentinel-1 and Sentinel-2 variables, showed a high R^2 value of 0.72 and a low RMSE of 0.143 for coconut trees, indicating strong predictive accuracy and statistical significance ($p<0.001$). This high level of performance makes the model reliable for estimating the AGB of coconut trees. With these results, Model 3 was utilized in the development of the equation for coconut using Equation 5 as the developed equation to predict AGB for coconut.

Table 6. Comparative analysis of model performance.

Model	R^2	RMSE (ton/pixel)	p
1	0.34	0.220	0.017
2	0.69	0.151	<0.001
3	0.72	0.143	<0.001
4	0.38	0.212	<0.001

$$\begin{aligned}\boldsymbol{Coconut\ Predicted\ AGB} &= 1.471 + 0.021 * VH\_Contrast) \\ &+ (0.037 * VH\_Dissimilarity) \\ &- (11.085 * B11) + (5.829 * B12) \\ &- (0.269 * CW) + (1.634 * FAPAR)\end{aligned} \quad \text{Equation 4}$$

3.5 Aboveground Biomass Map

The generation of the AGB was facilitated through the application of band math on the SNAP using Equation 5. Fig. 3 provides a visual representation of aboveground biomass distribution across the study area. Upon examination of the AGB map, it is evident that the aboveground biomass values exhibit a range from approximately 0.5 to 2 tons per pixel for coconut trees. The color gradient on the map ranges from green to orange, representing varying levels of AGB, which are measured in tons per pixel. Specifically, green areas indicate lower AGB values (around 0.51 tons per pixel), while orange areas indicate higher AGB values (up to 2.4 tons per pixel). Upon analyzing the map, it is observed that areas with higher AGB, marked in orange, correlate with locations where coconut trees are more densely packed. The field data used to create this map were collected from plots ranging in size from 6 to 9 trees per plot. This relatively small number of trees per plot can influence the accuracy of the AGB estimation. The distribution pattern seen in the map aligns with the expected distribution of coconut plantations in Butuan City, where denser clusters of trees result in higher aboveground biomass values. The observed AGB of coconut plantations in this study is 26 Megagrams per hectare (Mg/ha).

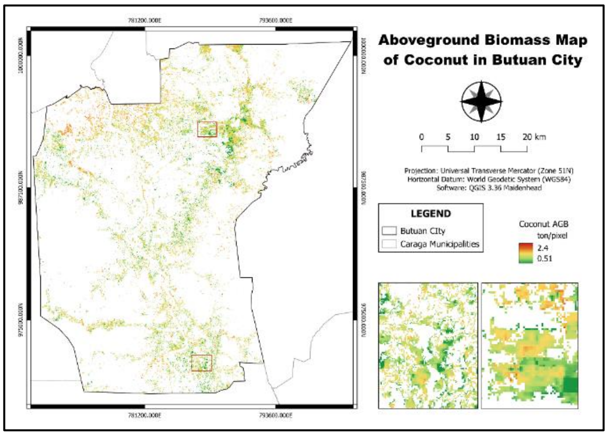

Fig. 3. Aboveground Biomass Map of coconut in Butuan City.

3.6 Carbon Stock Map

The carbon stock map for coconut (Fig. 4) exhibits a trend similar to that of the AGB maps, which is to be expected given that they are derived from AGB. A close examination of these maps reveals that the carbon stock values in the study area range from 0.2-1.15 tons per pixel. Upon conversion to a per-hectare basis, the carbon stocks amount to approximately 13 megagrams of carbon per hectare (MgC/ha). The carbon stocks calculated on a per-hectare basis amount to approximately 13 megagrams of carbon per hectare (MgC/ha), which is notably lower than values reported in previous studies. Kumar et al. [28] found an aboveground biomass (AGB) of 21.19 ± 1.23 Mg/ha, while Pragasan et al. [29] reported an AGB of 31.69 Mg/ha. Nur et al. [30] reported a carbon stock of 81.84 MgC/ha for trees, indicating higher carbon densities. However, Dey et al. [31] found a carbon content in coconut of 12.48 MgC/ha, which is somewhat consistent with the results in this study. The smaller carbon stock estimated in this study is likely influenced by the lower number of coconut trees per plot, which ranges from 6 to 9 trees. This lower density of trees per plot results in a reduced computed carbon stock compared to other studies.

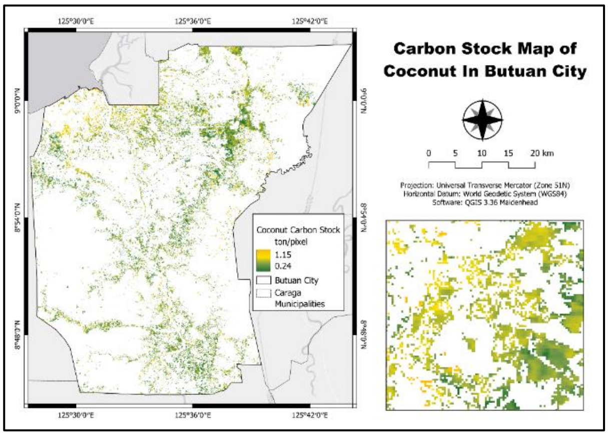

Fig. 4. Carbon Stock Map of coconut in Butuan City.

3.7 Accuracy Assessment of the Aboveground Biomass Map and Carbon Stock Map

The assessment compares AGB values obtained through field measurements with those predicted by remote sensing techniques across 12 plots. The residuals, indicating the difference between field measurements of coconut trees and remote sensing predictions, range broadly from -0.18 to 0.40 tons per pixel, with the mean residual being 0.21 tons per pixel. The average residuals resulted in RMSEs of 0.2783 tons per pixel (Fig. 5a).

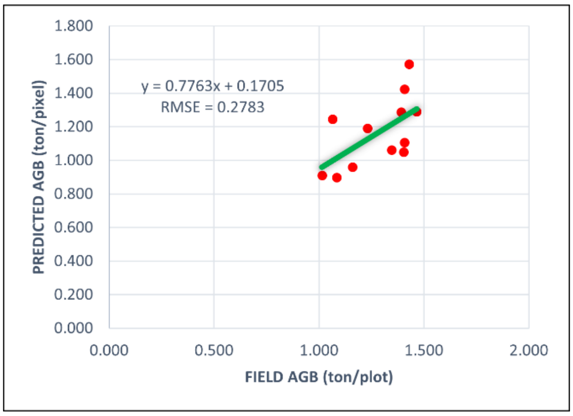

(a)

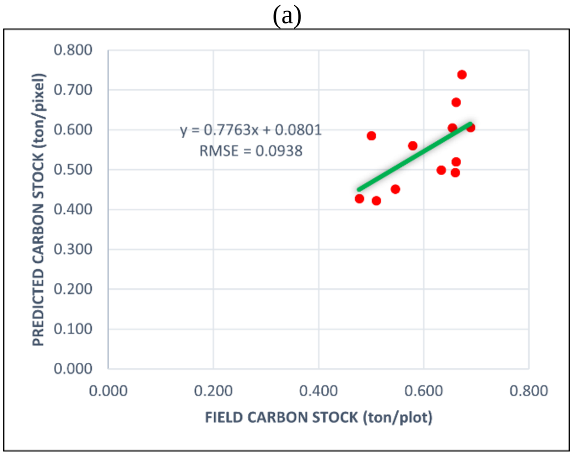

(b)

Fig. 5. Scatter plots showing (a) field AGB vs. predicted AGB, (b) field carbon stock vs. predicted carbon stock.

The calculated carbon stock values from field measurements for coconut trees vary across the plots, with values ranging from 0.477 to 0.689 tons per pixel, resulting in an average of 0.603 tons per pixel. On the other hand, the predicted carbon stock values from remote sensing data exhibit a spread from 0.423 to 0.739 tons per pixel, with a mean prediction of 0.549 tons per pixel. The residuals, representing the discrepancies between the calculated and predicted values, show both over- and underestimations, with a variance from -0.086 to 0.167, and an average of 0.055. The remote sensing techniques used for estimating carbon stocks of coconut trees in Butuan City show reasonable accuracy, with an RMSE of 0.0938 tons per pixel or 2.345 MgC/ha (Fig. 5b), indicating minor deviations from field measurements.

4. CONCLUSIONS AND RECOMMENDATIONS

In this study, Sentinel-1 and Sentinel-2 satellite imagery were utilized to estimate and map the AGB and carbon stock of coconut trees in Butuan City. The integration of SAR and optical remote sensing data resulted in a robust model with an R^2 value of 0.72 and a low RMSE of 0.143 for predicting AGB. The study reveals that the AGB of coconut in the study area is approximately 26 Megagrams per hectare (Mg/ha), while the aboveground carbon stock is about 13 megagrams of carbon per hectare (MgC/ha).

This high level of accuracy of carbon stock estimation for coconut, with RMSE of 0.0938 tons per pixel or 2.345 MgC/ha, can be attributed to the distinct structural characteristics of coconut trees, which are well captured by SAR data, and the specific spectral signatures identified by optical sensors. The consistency of the model's performance across both AGB and carbon stock predictions of coconut indicates that these remote sensing technologies effectively capture the necessary information for accurate biomass estimation.

Additionally, while remote sensing provides a wide-reaching perspective for assessing AGB, it can underestimate AGB due to several factors like Complex Vegetation Structures, which may not fully capture vegetation's vertical stratification and diverse tree forms, which is critical for precise AGB calculation. Also, data limitations where it might not accurately reflect understory vegetation or fine-scale tree density variations, which are significant for true AGB representation. Most important is the accuracy of allometric equations where AGB estimates depend on allometric equations that correlate tree measurements with aboveground biomass. Inaccuracies in these equations can introduce errors in AGB estimation. To enhance the robustness and applicability of the findings, it is advisable to expand the research scope to encompass a wider geographical area.

5. REFERENCES

[1] United Nations website: http://www.un.org/en/climatechange/what-is-climate-change/ (accessed 25.04.24).

[2] A. Mikhaylov, N. Moiseev, K. Aleshin, and T. Burkhardt, Global climate change and greenhouse effect, Entrepreneurship and Sustainability Issues, 7, 4 (2020) 2897-2913.

[3] UCDAVIS website: https://www.ucdavis.edu/climate/definitions/carbon-sequestration/ (accessed 27.04.24).

[4] University of Michigan News website: http://news.umich.edu/climate-change-threatens-

global-forest-carbon-sequestration-study-finds/ (accessed 27.04.24).
[5] DICF website: http://dicf.unepgrid.ch/philippines/forest/ (accessed 27.04.24).
[6] M. L. Bomhard, Palm Trees in the United States, University of Virginia: U.S. Department of Agriculture, Forest Service, 1963.
[7] CIFOR Forests News website: https://forestsnews.cifor.org/66546/survey-shows-potential-impact-of-palm-trees-in-quantifying-rainforest-carbon?fnl=en/ (accessed 27.04.24).
[8] W. L. M. E. Belem-Kabré, B. Kaboré, A. Compaoré-Coulibaly, T. K. Traoré, E. A. M. Thiombiano, M. Nebié-Traoré, M. Compaoré, F. B. Kini, S. Ouédraogo, M. Kiendrebeogo, and N. Ouédraogo, Phytochemical and biological investigations of extracts from the roots of *Cocos nucifera* L. (Arecaceae) and *Carica papaya* L. (Caricaceae), two plants used in traditional medicine, African Journal of Biochemistry Research, 15, 2 (2021) 28-35.
[9] M., Severino, Productive and Sustainable Coconut Farming Ecosystems as Potential Carbon "Sinks" in Climate-Change Minimization:A Review and Advisory Notes, 2011.
[10] M. R. Boston-Osoteo, A. J. B. Pontillo, and A. G. Apdohan, Utilization and evaluation of rice husk ash and coconut shell ash as partial cement replacement for concrete hollow blocks production, in Proceedings of International Exchange and Innovation Conference on Engineering & Sciences (IEICES), 8 (2022) 360-365.
[11] V. Pechanec, L. Štěrbová, J. Purkyt, M. Prokopová, R. Včeláková, O. Cudlín, P. Vyvlečka, E. Cienciala, P. Cudlín, Selected aspects of carbon stock assessment in aboveground biomass, Land, 11 (2022) 66.
[12] V.V. Namitha, S.K. Raj, K. Prathapan, Carbon Sequestration Potential in Coconut Based Cropping System: A Review. Agricultural Reviews (2022). DOI: 10.18805/ag.R-2553.
[13] V. Pechanec, L. Štěrbová, J. Purkyt, M. Prokopová, R. Včeláková, O. Cudlín, P. Vyvlečka, E. Cienciala, and P. Cudlín, Selected Aspects of Carbon Stock Assessment in Aboveground Biomass, Land, 11,1 (2022) 66.
[14] Y. Li, M. Li, and Y. Wang, Forest Aboveground Biomass Estimation and Response to Climate Change Based on Remote Sensing Data, Sustainability, 14, 21, (2022) 14222.
[15] S. Pandit, S. Tsuyuki, T. Dube, Estimating Above-Ground Biomass in Sub-Tropical Buffer Zone Community Forests, Nepal, Using Sentinel 2 Data, 10 (2018) 601.
[16] M. Salem and N. Tsurusaki, Empowering Sustainability: Innovative Deep Learning and Remote Sensing Solutions for Urban Monitoring and Sustainable Development, in Proceedings of International Exchange and Innovation Conference on Engineering & Sciences (IEICES), 9 (2023) 391-396.
[17] K. Kumar, M. Nagai, A. Witayangkurn, K. Kritiyutanont, and S. Nakamura, Above Ground Biomass Assessment from Combined Optical and SAR Remote Sensing Data in Surat Thani Province, Thailand, Journal of Geographic Information System, 8 (2016) 506-516.
[18] Caraga Region website: http://caragaregion.com/about-cities-and-provinces/butuan-city-home-of-the-balangays/ (accessed 25.04.24).
[19] T. Kavzoglu, F. Bilucan, and A. Teke, Comparison of support vector machines, random forest and decision tree methods for classification of sentinel-2A image using different band combinations, in Proc. 41st Asian Conf. Remote Sens. (ACRS 2020), 41 (2020) 1-8.
[20] K. Hairiah, S. Dewi, F. Agus, S. Velarde, A. Ekadinata, S. Rahayu, M. van Noordwijk, Measuring Carbon Stocks across Land Use Systems: A Manual, World Agroforestry Centre (ICRAF), SEA Regional Office, Bogor, (2010) 154.
[21] N. A. F. N. Effendi, N. A. M. Zaki, Z. A. Latif, M. N. Suratman, S. N. Bohari, M. Z. Zainal, H. Omar, Above-Ground Biomass and Carbon Stocks Estimation Using Allometric Equations in Tropical Forest, in Proc. ACRS 2020, 2020.
[22] Y. Ma, G. Jiang, J. Huang, Y. Shen, H. Guan, Y. Dong, J. Li, and C. Hu, Evaluating the ability of the Sentinel-1 cross-polarization ratio to detect spring maize phenology using adaptive dynamic threshold, Remote Sensing, 16, 5 (2024) 826.
[23] A. R. Zubair and O. A. Alo, Grey level co-occurrence matrix (GLCM) based second order statistics for image texture analysis, arXiv preprint arXiv:2403.04038, 2024.
[24] D. Zhao, J. Zhen, Y. Zhang, J. Miao, Z. Shen, X. Jiang, J. Wang, J. Jiang, Y. Tang, and G. Wu, Mapping mangrove leaf area index (LAI) by combining remote sensing images with PROSAIL-D and XGBoost methods, Remote Sensing in Ecology and Conservation, 9, 3 (2023) 370-389.
[25] W. Li, M. Weiss, F. Waldner, P. Defourny, V. Demarez, D. Morin, O. Hagolle, F. Baret, A Generic Algorithm to Estimate LAI, FAPAR and FCOVER Variables from SPOT4_HRVIR and Landsat Sensors: Evaluation of the Consistency and Comparison with Ground Measurements, Remote Sensing, 7, 11 (2015) 15494-15516.
[26] A. Elsherif, R. Gaulton, J. Mills, and E. Sharaf El Din, Measuring Forest canopy water mass in three dimensions using terrestrial laser scanning, Int. Arch. Photogramm. Remote Sens. Spatial Inf. Sci., XLVIII-1/W2 (2023) 721-726.
[27] S. Muhe and M. Argaw, Estimation of above-ground biomass in tropical afro-montane forest using Sentinel-2 derived indices, Environ Syst Res, 11, 5 (2022).
[28] B. M. Kumar and D. Balasubramanian, Carbon stocks of forests and tree plantations along an elevational gradient in the Western Ghats: Does plant diversity impact forest carbon stocks?, Anthropocene Science (2024).
[29] L. A. Pragasan and M. Kalaiselvi, Carbon stock potential of coconut plantations in university campus: A case study from Coimbatore, India, Asian Journal of Research in Agriculture and Forestry, 10, 2 (2024) 140-146.
[30] A. Nur, K. Arifiani, A. Ramadhani, A. Sabrina, G. Dwi Nugroho, L. Kusumaningrum, D. Ramdhun, T.

Bao, C. Yap, S. Budiharta, and A. Setyawan, Estimation of aboveground biomass and carbon stock in Damas Beach, Trenggalek District, East Java, Indonesia, Indo Pac. J. Ocean Life, 6 (2022) 80-86.
[31] A. Dey, M. Islam, and K. Masum, Above ground carbon stock through palm tree in the homegarden of Sylhet City in Bangladesh, J. Forest Environ. Sci., 30 (2014) 293-300.